SEISMIC LOSS ESTIMATION OF R/C STRUCTURES BASED ON A GEOMETRICAL DAMAGE MODEL

Noriyuki TAKAHASHI[1] and Yoshiaki NAKANO[2]

ABSTRACT: To evaluate visible damage of reinforced concrete (R/C) members such as crack width and length, cyclic load tests of one third scaled R/C members were carried out. Based on the tests, a geometrical damage estimation model is proposed to quantify each crack width and corresponding length. The model consists primarily of a geometrical condition for the relationship between the sum of crack widths and drift ratio and a probabilistic model between crack widths and lengths. Applying the proposed model to seismic response analyses of R/C building structures modeled as fish-bone shaped frames, the damage and repairing process, as well as life cycle economic loss were simulated. Life cycle economic loss was defined here as the repairing cost for maintenance of the functionality of a building through its life length. As a result, it is implied that the case of main damages on beams will suffer more life cycle economic losses than the case of main damages on columns because of the extent of damaged area and the construction cost of falsework.

***Key Words**: Crack widths; Crack length; Damage quantification; Life-cycle economic loss*

INTRODUCTION

Loss estimation of a building due to earthquake events in its life length is important to facilitate the decision making of the building owner to choose the reasonable seismic performance. Generally it is assumed that the visible damage of reinforced concrete (R/C) members such as crack width and length are subjected to one of principal components for seismic loss (e.g. structural repair cost) estimation. In this paper, the visible damage is modeled as a geometrical relationship between the sum of crack widths and drift ratio and a probabilistic model between crack widths and lengths based on the cyclic load tests of one third scaled R/C members. And the life cycle economic loss defined as the repairing cost of a building structure through its life length was simulated using the proposed model.

[1] Research Associate, Institute of Industrial Science, The University of Tokyo
[2] Professor, Institute of Industrial Science, The University of Tokyo

EXPERIMENTAL PROGRAM

Test specimens, setup and instrumentation

Two R/C beam specimens proportioned to approximately 1/3 of full scale were tested under cyclic loading. The design parameters and corresponding values are given in Table 1. The dimension for the test specimens and test setup are shown in Fig. 1 and 2. To obtain the propagation of crack width and length corresponding to attained and present drift ratio, the cyclic displacement pattern shown in Fig. 3 was operated. Crack widths were measured at the points shown in Fig. 4. Crack lengths were measured by image processing of sketched cracking pattern.

Table 1 Description of test specimens

Specimen	Concrete Strength (N/mm^2)	Rebar - Tensile reinforcement ratio to the section	Yield strength of rebar (N/mm^2)	Lateral reinforcement - Lateral reinforcement ratio to the section	Yield strength of lateral reinforcement (N/mm^2)	Failure mode
F-1	30	8-D13 - 0.0121	295	D4@60 - 0.0022	295	Flexure
S-1	18		785		295	Shear

D: diameter of deformed bar

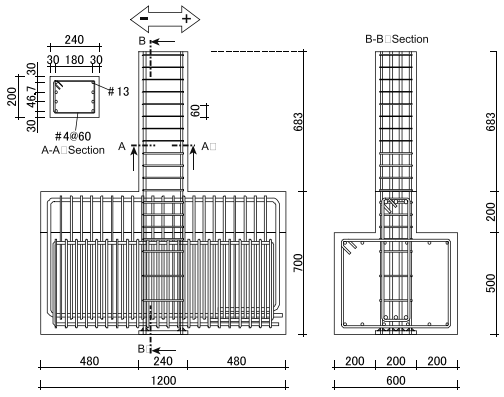

Fig. 1 Dimension of beam specimen

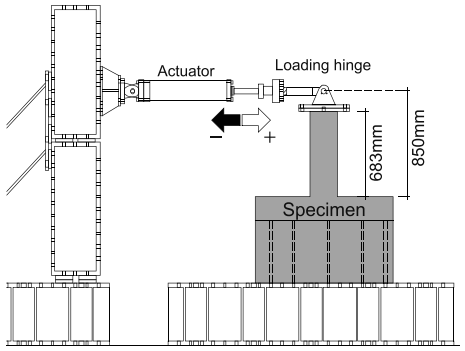

Fig. 2 Test setup

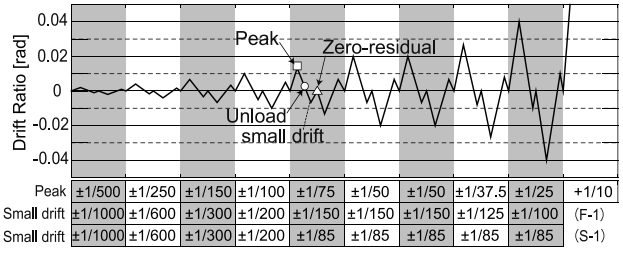

Peak	±1/500	±1/250	±1/150	±1/100	±1/75	±1/50	±1/50	±1/37.5	±1/25	+1/10
Small drift	±1/1000	±1/600	±1/300	±1/200	±1/150	±1/150	±1/150	±1/125	±1/100	(F-1)
Small drift	±1/1000	±1/600	±1/300	±1/200	±1/85	±1/85	±1/85	±1/85	±1/85	(S-1)

Fig. 3 Cyclic displacement pattern

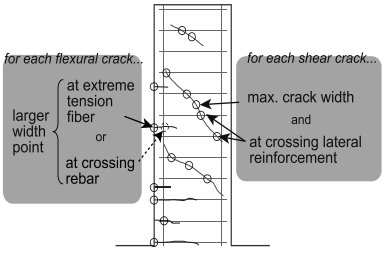

Fig. 4 Crack measurement point

Test results

Fig. 5 shows the shear force versus drift response for each specimen and the cracking pattern at 4.0% drift. Measured maximum and average crack widths are shown in Fig. 6. Measured crack lengths are shown in Fig. 7. Specimen F-1 designed to fail in flexure opened existing cracks due to increase in drift ratio instead of generating new cracks after yielding. Therefore total crack length did not increase significantly. On the other hand, Specimen S-1 designed to fail in shear generated new cracks due to the increase in drift ratio after yielding. Crack length as well as crack width increased. Crack width and length of specimen S-1 increased rather than specimen F-1 in large drift.

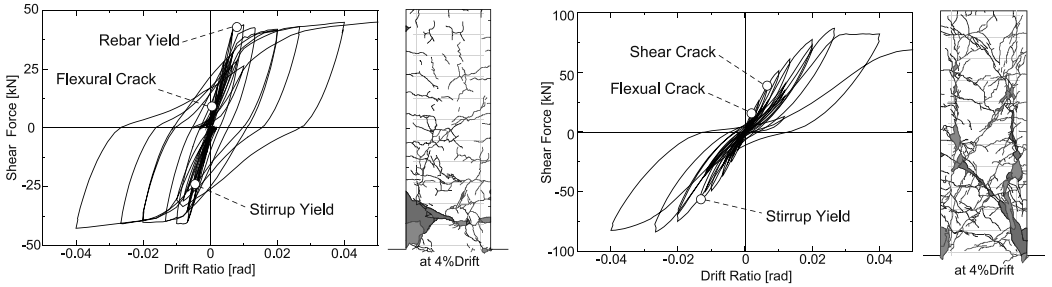

(a) Specimen F-1 (b) Specimen S-1

Fig. 5 Shear force versus drift ratio response, and cracking pattern

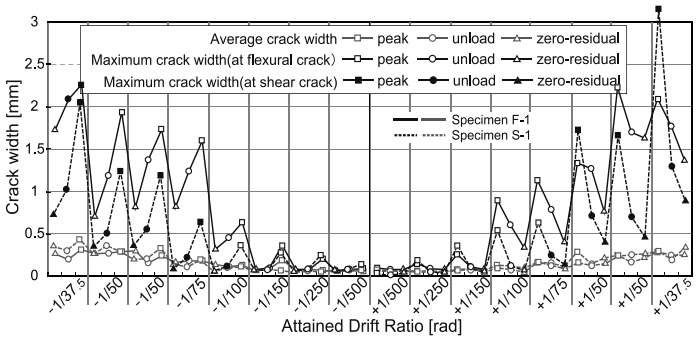

Fig. 6 Crack width for attained drift ratio

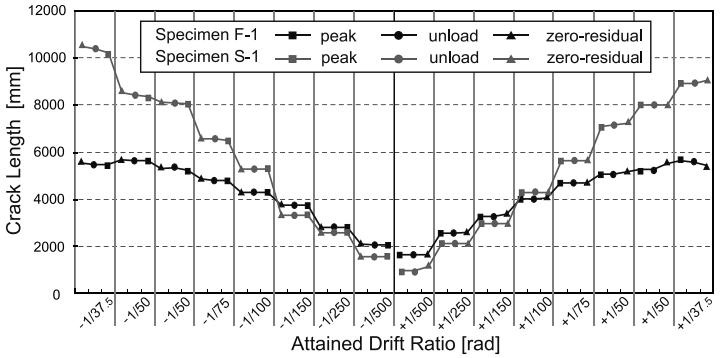

Fig. 7 Crack length for attained drift ratio

DAMAGE ESTIMATION

Geometrical damage estimation model

Residual crack width has been regarded as a key factor of quantfying the structural damage (Maeda, et al., 2004, Maeda, et al., 2009, and etc.). But in many case, residual crack width expediently relates not to the residual drift after excitation but to the attained maximum drift. In this paper, geometrical macro model of relation between crack width and drift ratio shown in Fig. 8 (AIJ 2004) is applied to estimating the residual crack width after excitation. The relation between crack width and drift ratio is expressed as

$$R = R_f + R_s = \frac{\sum w_f}{D - x_n} + \frac{2\sum w_s \cdot \cos\theta}{L} \tag{1}$$

in which R_f: current flexural drift ratio, R_s: current shear drift ratio, w_f: flexural crack width, w_s: shear crack width, D: depth, x_n: distance from extreme compression fiber to neutral axis, and L: clear span, respectively. Eq. (1) considers the experimental result of shear crack width and shear drift shown in Fig. 9, which is proposed by Sugi, et al., (2007).

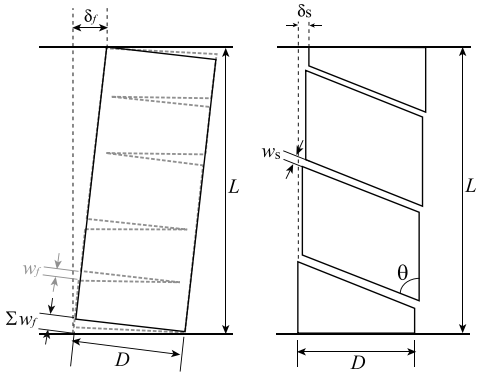

Fig. 8 Geometrical model between crack width and drift

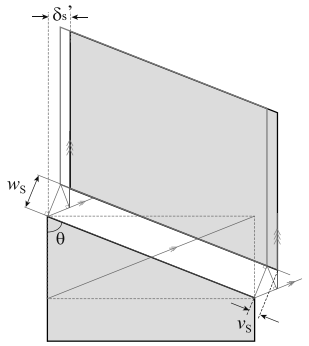

Fig. 9 Geometrical model between shear crack width and shear drift based on experimental results

CEB-FIP (1978) proposed crack spacing shown in Fig. 10. Crack length at stabilized crack pattern due to Fig. 10 is expressed as

$$l_{av,f} = \frac{\zeta \cdot L \cdot (D - x_n)}{S_{av}} \tag{2-1}$$

$$l_{av,s} = \frac{D}{\sin\theta}\left(\frac{D\cos\theta + L\sin\theta}{S_{av}} - 2q\right) + \frac{q \cdot (q+1) \cdot S_{av}}{\sin\theta\cos\theta} \tag{2-2}$$

in which $l_{av,f}$: stabilized flexural crack length, $l_{av,s}$: stabilized shear crack length, ζ: dimensionless parameter representing the crack propagation, S_{av}: crack spacing, θ: crack angle, and q: quotient of $D\cos\theta$ / S_{av}, respectively.

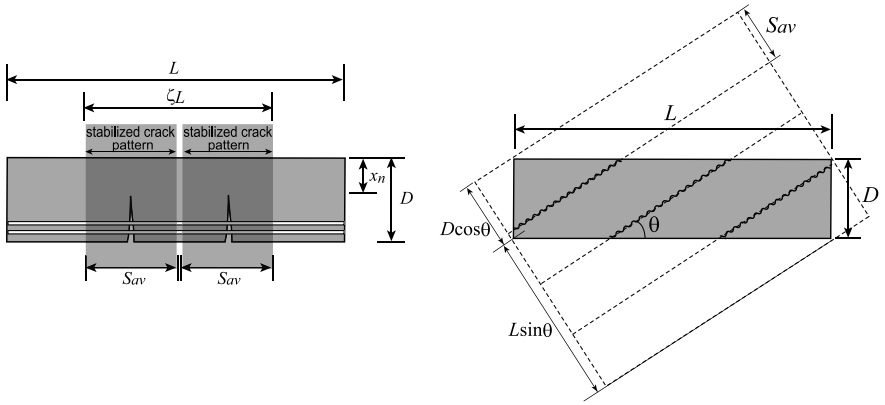

(a) Flexural crack spacing (b) Shear crack spacing

Fig. 10 Crack spacing

Estimation results of the maximum crack width, which is selected from larger one of the maximum flexural crack width and the maximum shear crack width, are shown in Fig. 11 to 12. Likewise, estimation results of the total crack length are shown in Fig. 13. It is assumed that the crack width can be calculated from the residual drift after excitation with the geometrical model. The estimated crack width of specimen F-1 can approximately simulate the experimental result. On the contrary, that of specimen S-1 can approximately simulate the experimental result only at the unloaded drift, and it overestimates at the peak drift and underestimates at the zero-residual drift. It implies that the geometrical model shown in Fig. 7 matches up with the unloaded drift condition. Based on Fig. 13, crack length propagation model is proposed in Fig. 14. In Fig. 14, β means the ratio of flexural drift to total drift. Additionally, spalling propagation model is proposed in Fig.15 based on previous research (Takahashi, et al., 2009) though it depends not on the geometrical model but on the empirical model. It is formulated as

$$SR = \alpha_{sp} \times (IDR_{max} - R_0) \tag{3}$$

where, SR: spalling ratio [m^2/m^2], α_{sp}: constant value (= 3.67), R_0: initial spalling drift ratio (= 0.01 rad.), and IDR_{max}: attained maximum drift ratio. In the next section, a new probabilistic model between crack widths and lengths is introduced.

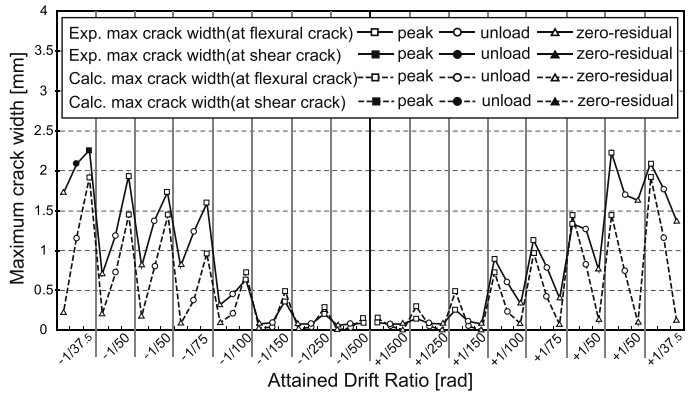

Fig. 11 Crack width estimation of specimen F-1

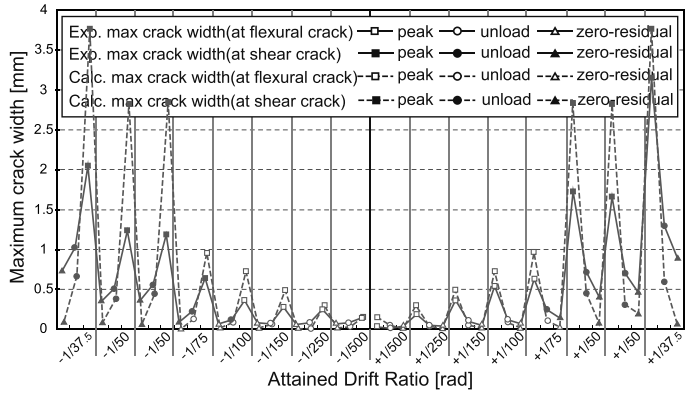

Fig. 12 Crack width estimation of specimen S-1

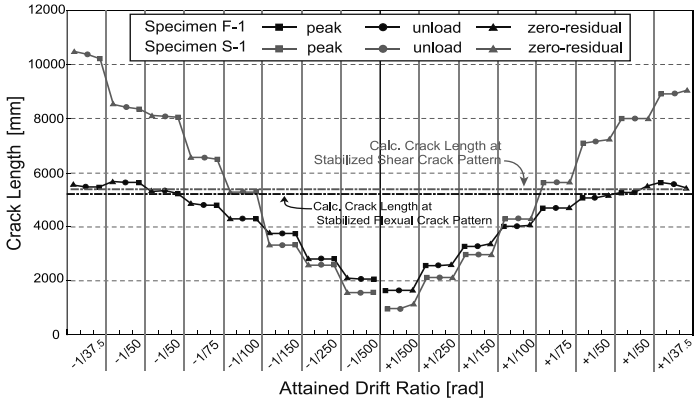

Fig. 13 Stabilized crack length estimation

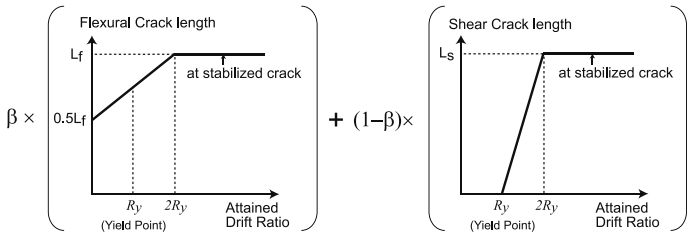

Fig. 14 Crack length propagation model

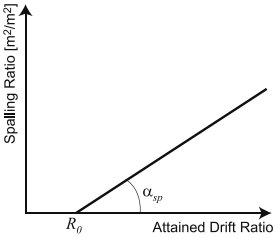

Fig. 15 Spalling model

Probabilistic Model between crack width and length

Crack width and crack spacing, which could convert into crack length, can be predicted by numerical models proposed in recent researches (Avril, et al., 2005, Winkler, et al., 2004, and etc.). These approaches are often used in finite element method and the finite element mesh should be a key factor to calculate the crack width and crack length converted from crack spacing. On the contrary, a probabilistic model between crack widths and lengths is introduced in this study to handle the macro-model such as a geometrical damage estimation model easier than finite element method. Crack length distribution to crack width is represented as log-normal distribution in this model based on the previous research (Takimoto, et al., 2004). Fig. 16 and 17 show the crack length distribution histograms at the drift of 0.002, 0.004, 0.01, 0.02 rad., respectively. As concern with the standard deviation, the experimental results are shown in Table 2. The obtained values of σ from the experimental tests are around 0.61~1.40 when a natural logarithm are used as a random variable of log-normal distribution. The average value of σ is 1.2 after yielding, which corresponding attained drift is over 0.0067 rad. in specimen F-1 and over 0.013 rad. in specimen S-1.

Using the crack widths estimated by the geometrical model and the standard deviation σ obtained from the experimental tests, the crack length distribution histograms at the attained drift ratio of 0.002, 0.004, 0.01, 0.02 rad. are calculated. The calculated results are overwritten in Fig. 16 and 17.

The calculated crack length distribution histograms of specimen F-1 approximately simulate the experimental results at small drift stage. But the trends for underestimating the crack length of a smaller crack width at the peak drift stage and overestimating the crack length of a smaller crack width at the zero-residual drift stage are shown in Fig. 16 according to the increase of attained drift.

The calculated crack length distribution histograms of specimen S-1 approximately simulate the experimental results at small drift stage. Also the trends for underestimating the crack length of a smaller crack width at the peak drift stage and overestimating the crack length of a smaller crack width at the zero-residual drift stage are shown in Fig. 17 according to the increase of attained drift.

Table 2 Standard deviation of crack length distribution obtained from experimental tests

	Attained drift 0.002[rad.]			Attained drift 0.004[rad.]			Attained drift 0.01[rad.]			Attained drift 0.02[rad.]		
	peak	unloaded	zero-residual	peak	unloaded	zero-residual	peak	unloaded	zero-residual	peak	unloaded	zero-residual
F-1	0.70	0.70	0.65	0.75	0.79	0.80	1.01	0.97	1.05	1.34	1.35	1.26
S-1	0.83	0.83	0.84	0.62	0.70	0.61	0.90	0.94	0.65	1.31	1.40	1.30

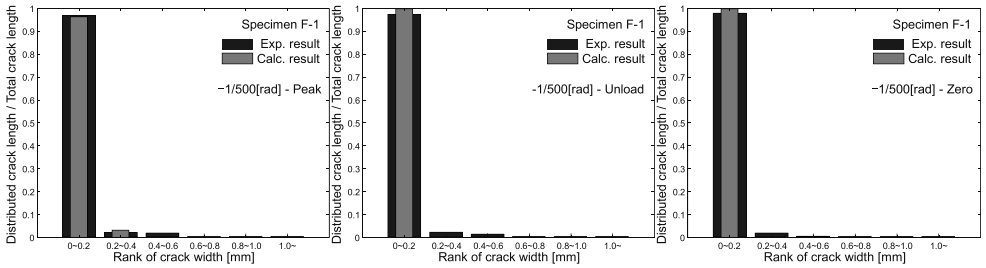

(a) At the attained drift ratio = 0.002 rad. (Peak, Unloaded, Zero-residual drift stage, respectively)

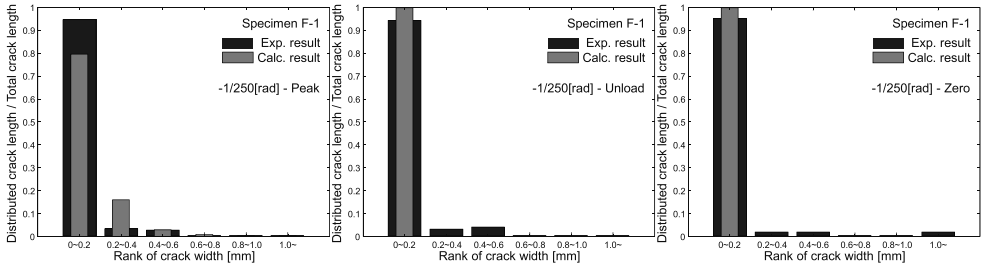

(b) At the attained drift ratio = 0.004 rad. (Peak, Unloaded, Zero-residual drift stage, respectively)

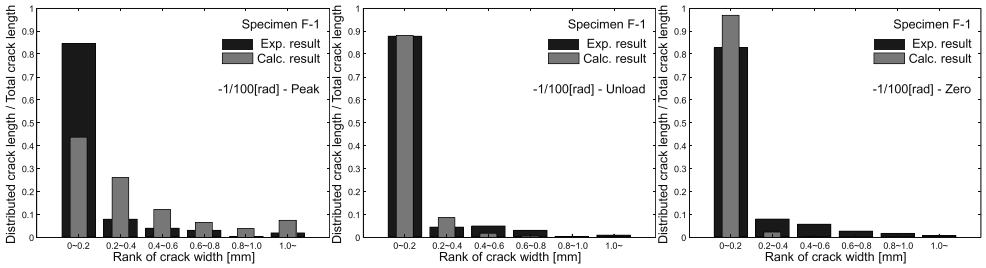

(c) At the attained drift ratio = 0.01 rad. (Peak, Unloaded, Zero-residual drift stage, respectively)

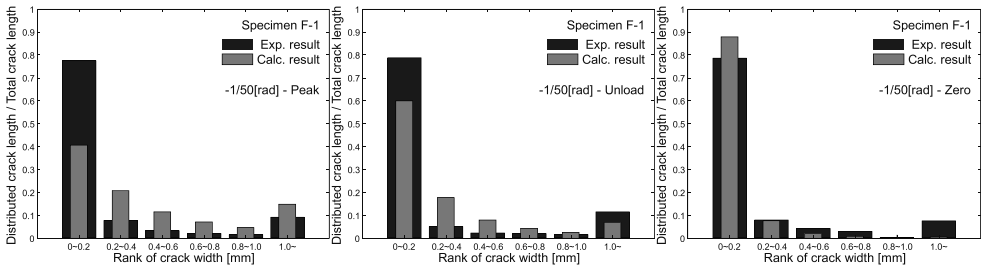

(d) At the attained drift ratio = 0.02 rad. (Peak, Unloaded, Zero-residual drift stage, respectively)

Fig. 16 Crack length distribution to crack width (Specimen F-1)

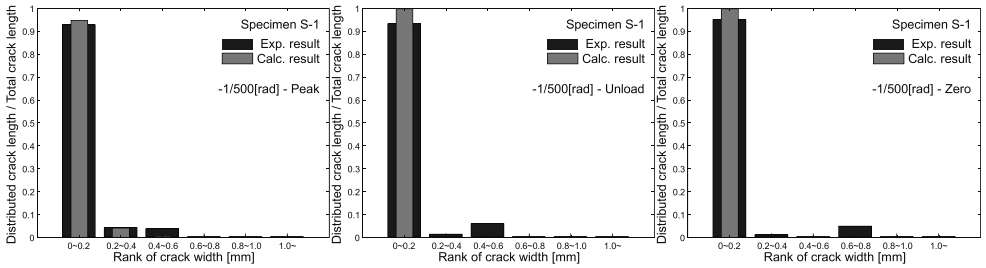

(a) At the attained drift ratio = 0.002 rad. (Peak, Unloaded, Zero-residual drift stage, respectively)

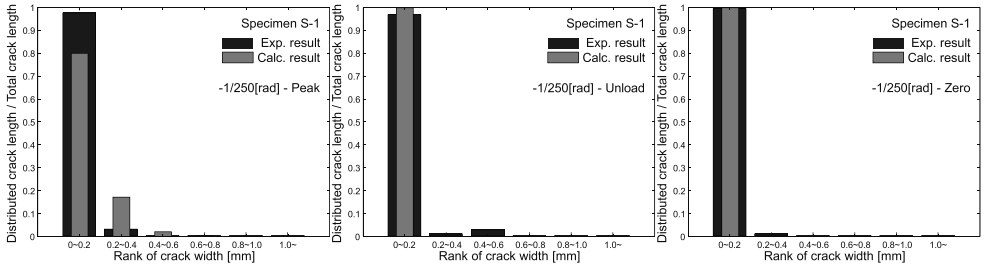

(b) At the attained drift ratio = 0.004 rad. (Peak, Unloaded, Zero-residual drift stage, respectively)

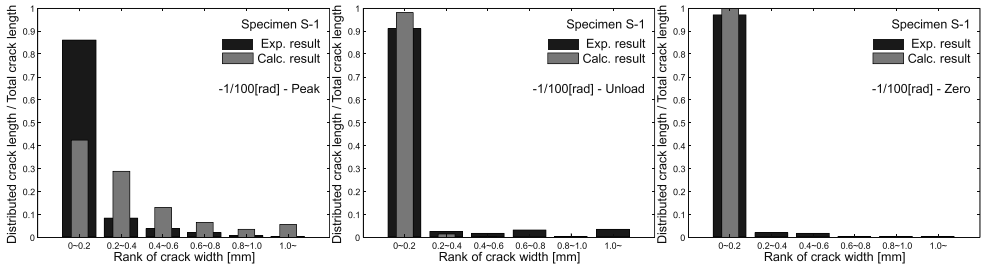

(c) At the attained drift ratio = 0.01 rad. (Peak, Unloaded, Zero-residual drift stage, respectively)

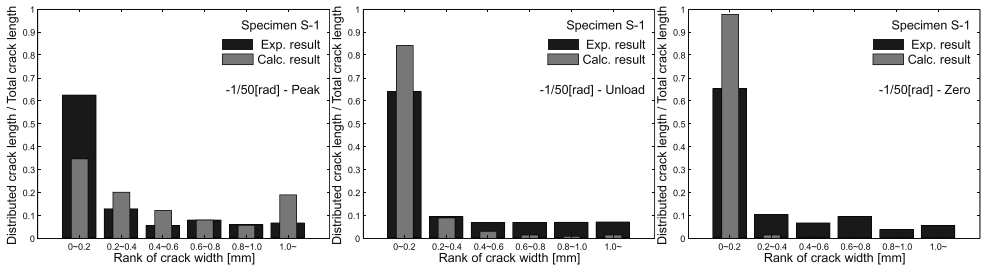

(d) At the attained drift ratio = 0.02 rad. (Peak, Unloaded, Zero-residual drift stage, respectively)

Fig. 17 Crack length distribution to crack width (Specimen S-1)

LIFE-CYCLE SEISMIC LOSS ESTIMATION

Outline

Several loss estimation models (Onur, et al., 2002, NIBS/FEMA 2003, and etc.) have been proposed based on a fragility curve through vulnerability analysis (Rosseto, et al., 2003, and etc.). But whenever the sample of vulnerability analysis is changed, a fragility curve needs to be reconstructed. In this study, a deterministic procedure without a fragility curve is applied to calculate the seismic loss.

To estimate the seismic loss of a building constructed in high seismic zone, damage due to medium to major earthquakes is not negligible. Then life-cycle seismic loss would be a good measurement to estimate the reparability performance in high seismic zone. Life-cycle seismic loss is defined as a total repair cost of a building expected in its life length.

Input ground motion

Based on the seismic hazard curve proposed by National research Institute for Earth science and Disaster prevention (NIED 2009), Fig. 18 is obtaind as peak velocities of ground motion on engineering bedrock in Tokyo. Enhancing the plotting position equation (Takahashi, et al., 2009), a series of peak velocities through lifecycle is created in Fig. 19. And four artificial earthquake motions are generated such that they should fit the design spectra defined by the cabinet order of the Minister of Land, Infrastructure and Transport (MLIT) Government of Japan, while the phase characteristic of Kobe 1995 (NS), El Centro 1940 (NS), Hachinohe 1968 (EW), and Tohoku Univ. 1978 (NS) are used. They are factored such that their peak velocities should match to each of the four target peak ground velocities in Fig. 19.

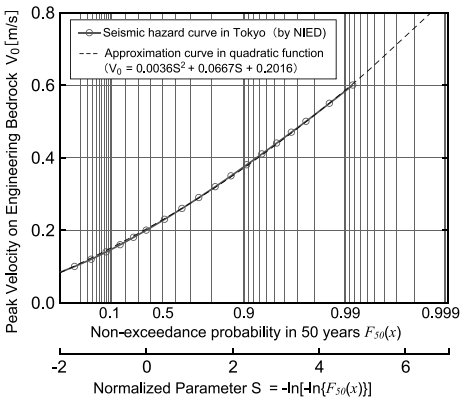

Fig. 18 Seismic hazard curve in Tokyo

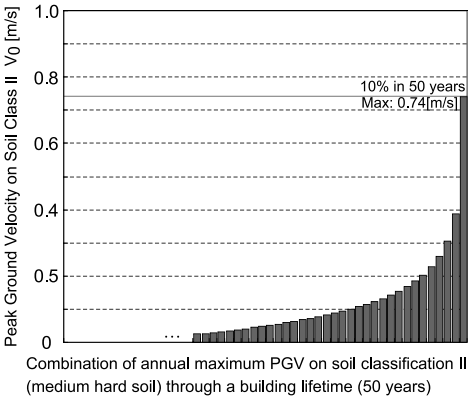

Fig. 19 Example of life-cycle PGV

Structural Model

Two fishbone-shaped frames shown in Figure 20 are studied for estimating the life cycle repair cost. One is strong-column and weak-beam frame with beam rebar strength σ_s=390N/mm^2. Another is weak-column and strong-beam frame with beam rebar strength σ_s=490N/mm^2. Takeda hysteresis model (Takeda, et al., 1970) is used for each member modeled as one-component model. Viscous damping factors proportional to instantaneous stiffness are assumed to be 3%. The cracking strength is assumed to be one third of yielding strength, the secant stiffness at yielding point is assumed to be

30% of the linearly elastic stiffness, and the third stiffness after yielding is assumed to be 1% of the linearly elastic stiffness for each member.

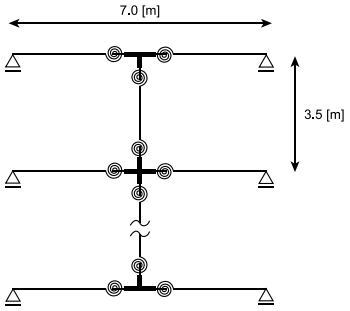

Common Variable:
Mass : 11.8 kN/m^2
Column : 700mm×700mm (Fc32, 8-D32/ σ_s=390N/mm^2)
Beam : 400mm×800mm (Fc24, 8-D25/ σ_s=*)
Footing : 600mm×1800mm (Fc32, 12-D32 / σ_s=390N/mm^2)

*Analytical Parameter:
(a) Strong-column and weak-beam type
Beam rebar strength: σ_s=390N/mm^2
(b) Weak-column and strong-beam type
Beam rebar strength: σ_s=490N/mm^2

Fig. 20 Structural model

Repairing Policy Scenario and repairing cost model

Providing the maximum drift ratio is larger than yielding drift (assumed to be 0.067 rad. in this study), structures are repaired according to the scenario described in Table 3. If the maximum displacement is smaller than yielding drift, structures are left unrepaired with damage such as stiffness degradation.

Table 3 Repairing scenario

Condition	Repair method		Unit price
Crack width < 0.2mm	Sealing		\$9.1 /m
Crack width < 1.0mm	Epoxy injection		\$66.0 /m
Crack width ≥ 1.0mm	U-cut sealing / Cement grout		\$125.4 /m
Spalling ratio < 0.05	Patching resin mortar		\$270.0 /m^2
Spalling ratio ≥ 0.05	Jacketing / Replacement		\$542.3 /m^2
at Interior Column	No falsework		\$20.0 /m^2
at Interior Beam	False-work height	Half floor height	
at Exterior Column		Damaged floor level	
at Exterior Beam		Damaged floor level+ half floor height	

Analytical results

Estimated life cycle economic losses of two structures defined as the repairing cost of structures through their life length are shown in Fig. 21. Life cycle economic loss due to repairing the cracks are higher in the strong-column and weak-beam structure than the weak-column and strong beam structure, but life cycle economic loss due to repairing the spalling are higher in the weak-column and strong beam structure than the strong-column and weak-beam structure.

Repairing cost of spalling depends on the maximum inter-story drift ratio through the life length. As shown in Fig. 22, the maximum inter-story drift ratio, which come out at the 2nd floor, is larger in the weak-column and strong beam structure than the strong-column and weak-beam structure. On the contrary, repairing cost of cracking depends not on the maximum drift ratio in specified-story but on the sum of drift ratio in all stories. The strong-column and weak-beam structure shows the smaller maximum drift ratio at the 2nd floor, but its drift ratio at the other floor is larger than that of the weak-column and strong beam structure. This extent of cracking area affects the repairing cost of

cracking. Life cycle economic loss due to falsework is larger in the case of the exterior frame or the strong-column and weak-beam structure because of the extent of damaged area.

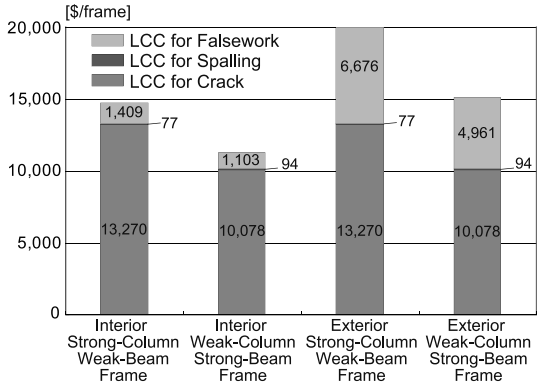

Fig. 21 Calculated life-cycle economic loss

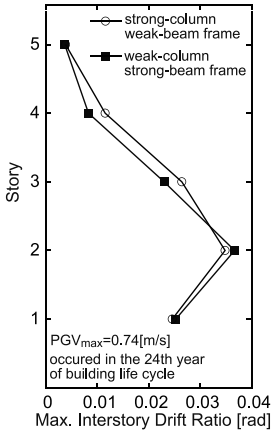

Fig. 22 Maximum IDR

CONCLUDING REMARKS

To estimate the reparability performance of a building including nonstructural components through its life cycle, the estimation model of visible damage, such as crack width and length, and the estimation method of life-cycle seismic loss were proposed. And the procedure to calculate the life-cycle seismic loss was demonstrated by very simple examples. It is revealed that the extent of cracking area affects the repairing cost of cracking. And the life cycle economic loss due to falsework is larger in the case of the exterior frame or the strong-column and weak-beam structure because of the extent of damaged area.

REFERENCES

Architectural Institute of Japan (2004), *Guidelines for Performance Evaluation of Earthquake Resistant Reinforced Concrete Buildings (Draft)* (in Japanese)

Avril S., Vautrin A., Hamelin P., and Surrel Y. (2005), "A multi-scale approach for crack width prediction in reinforced-concrete beams repaired with composites", *Journal of Composites Science and Technology*, 65, 445-453.

CEB-FIP (1978), *Model Code for Concrete Structures*

Maeda M., Nakano Y., and Lee K. S. (2004), "Post-Earthquake Damage Evaluation for R/C Buildings based on Residual Seismic Capacity", *Proceedings of the 13th World Conference on Earthquake Engineering*, Paper No.1179.

Maeda M. and Kang D. E. (2009), "Post-Earthquake Damage Evaluation of Reinforced Concrete Buildings", *Journal of Advanced Concrete Technology*, Vol. 7, No. 3, 327-335.

NIED (2009), *National seismic hazard maps for Japan* (in Japanese)

NIBS/FEMA (2003), *Multi-Hazard Loss Estimation Methodology: Earthquake Model, HAZUS-MHMR1 Technical Manual, HAZUS99-SR2*

Onur T., Ventura C. E. and Finn W. D. L. (2002), "Seismic damage estimation in southwestern British Columbia", *Proceedings for Seventh U.S. National Conference on Earthquake Engineering*, Paper ID: LE-2f

Rosseto T. and Elnashai A. (2003), "Derivation of vulnerability functions for European-type RC structures based on observational data", *Journal of Engineering Structures,* 25*,* 1241-1263.

Sugi T., Ishimori A., Tajima k., and Shirai N. (2007), "Damage evaluation of RC beam members based on accurate measurement of displacement and crack widths with scanner (part 2) proposal of rational suggestion of quantitative evaluation model for evaluating of shear crack width – shear deformation relationship", *Summaries of Technical Papers of Annual Meeting of Architectural Institute of Japan,* C-2, 373-374 (in Japanese)

Takahashi N. and Nakano Y. (2009), "A Study on seismic repair cost of R/C building structures using a geometrical damage estimation model of R/C members", *Proceedings of the Eighth International Symposium on New Technologies for Urban Safety of Mega Cities in Asia*, 313-322.

Takeda T., Sozen M. A. and Nielsen N. N. (1970), "Reinforced concrete response to simulated earthquakes", *Journal of Structural Division*, *ASCE*, 96: ST12, 2557-2573.

Takimoto, K. et al. (2004) "Study on evaluation of damage of RC beams using crack data", *Journal of the Japan Society of Civil Engineers*, 760/V-63, 135-145. (in Japanese)

Winkler B., Hofstetter G., and Lehar H. (2004), "Application of a constitutive model for concrete to the analysis of a precast segmental tunnel lining", *International Journal for Numerical and Analytical Methods in Geomechanics,* 28*,* 797-819.